

## SIMULTANEOUS X-RAY AND OPTICAL OBSERVATIONS OF GX 339-4 IN AN X-RAY HIGH STATE

K. MAKISHIMA, Y. MAEJIMA<sup>1</sup>, AND K. MITSUDA  
 Institute of Space and Astronautical Science, Tokyo

H. V. BRADT AND R. A. REMILLARD  
 Center for Space Research, Massachusetts Institute of Technology

I. R. TUOHY  
 Mount Stromlo and Siding Spring Observatories, Australian National University

R. HOSHI  
 Department of Physics, Rikkyo University, Tokyo

AND

M. NAKAGAWA  
 Department of Physics, Osaka City University, Osaka  
 Received 1985 August 29; accepted 1986 February 28

### ABSTRACT

The black hole candidate GX 339-4 (4U 1658-48) was observed simultaneously in X-rays and visible light, using the X-ray satellite *Tenma* and the 1.0 m telescope at Siding Spring Observatory. The Anglo-Australian Telescope was also used. The object was in a typical high state in X-rays. The optical counterpart was moderately bright ( $V \approx 16.4$ ), but fainter by  $\sim 1$  mag than in the X-ray low state in 1981. No fast time variation was found either at X-ray or optical wavelengths. The X-ray spectrum comprised a very soft component with a characteristic temperature of about 0.77 keV, and a hard tail having a power-law photon slope of about 2. The hard tail intensity increased gradually with time, while the soft X-ray component was very stable, and agrees well with radiation expected from an optically thick accretion disk. We obtained an X-ray (2-10 keV) to optical (300-700 nm) energy flux ratio of about 140, assuming  $A_v = 2.5$ . These results are interpreted in terms of a mass-accreting black hole of about  $3 M_\odot$ .

*Subject headings:* black holes — stars: individual — X-rays: binaries — X-rays: spectra

### I. INTRODUCTION

In spite of attempts by many investigators to search for stellar-mass black holes, only a handful of candidates have so far been found. The X-ray source GX 339-4 (4U 1658-48) is one such example, in addition to Cyg X-1 (Oda 1977; Liang and Nolan 1984), Cir X-1 (e.g., Dower, Bradt, and Morgan 1982), LMC X-3 (Cowley *et al.* 1983; White and Marshall 1984), LMC X-1 (Hutchings, Crampton, and Cowley 1983), SS 433 (Margon 1984) and A0620-00 (McClintock and Remillard 1986). The X-ray behavior of GX 339-4 has been studied from various satellites, including *OSO 7* (Markert *et al.* 1973), *HEAO 1* (Samimi *et al.* 1979; Nolan *et al.* 1982), *Hakucho* (Maejima *et al.* 1984, hereafter Paper I) and *Ariel 6* (Motch *et al.* 1983; Ricketts 1983). GX 339-4 may be found either in "high," "low," or "off" states in X-rays (Markert *et al.* 1973). The X-ray spectrum steepens in the high state (Ricketts 1983). In the low state the X-ray spectrum is much flatter, and the X-ray intensity exhibits random fast ( $< 1$ ) variations.

GX 339-4 has been identified optically with a variable faint object (Doxsey *et al.* 1979; Grindlay 1979). The optical faintness during the X-ray off state and a large range of optical variation ( $V = 15.4-21$ ) imply a low-mass optical counterpart, and the optical emission seems a direct consequence of mass accretion onto the compact object (Paper I; Motch *et al.* 1983) rather than coming from the companion star. GX 339-4 therefore provides us with a unique opportunity to study both the optical and X-ray emission due to accretion by an object

that is a black hole candidate. Simultaneous X-ray and optical observations are thus particularly important in studying GX 339-4.

Motch, Ilovaisky, and Chevalier (1982, hereafter MIC) detected peculiar optical activity of GX 339-4 during a low state in 1981 May. Simultaneous optical/X-ray observations on the same occasion (Motch *et al.* 1983) revealed an intensity anticorrelation between these two frequencies. Soon after, *Hakucho* observed the source transition from the low to high state, and the short-term X-ray variation disappeared after the transition. These recent X-ray and optical observations have deepened our understanding of GX 339-4 and reinforced its black hole candidacy. In fact, the overall X-ray and optical properties of GX 339-4 are quite alien to those of neutron-star binaries, while it shares most of its X-ray characteristics in common with Cyg X-1, the leading black hole candidate (see Paper I).

We observed GX 339-4 simultaneously at X-ray and optical frequencies, using the X-ray satellite *Tenma*, and the 1.0 m telescope at Siding Spring Observatory. High quality X-ray spectra were obtained with the Gas Scintillation Proportional Counters (GSPC) on board *Tenma*. In addition, a brief optical spectrum was obtained on the Anglo-Australian Telescope (AAT) just after the completion of the simultaneous observations. The source was found in a typical X-ray high state, while the optical counterpart was moderately bright ( $V \approx 16.4$ ). This appears to be one of the first reports of simultaneous optical and X-ray observations of GX 339-4 during the X-ray high state (see also MIC and Motch *et al.* 1984). The object showed

<sup>1</sup> Nippon Electric Company.

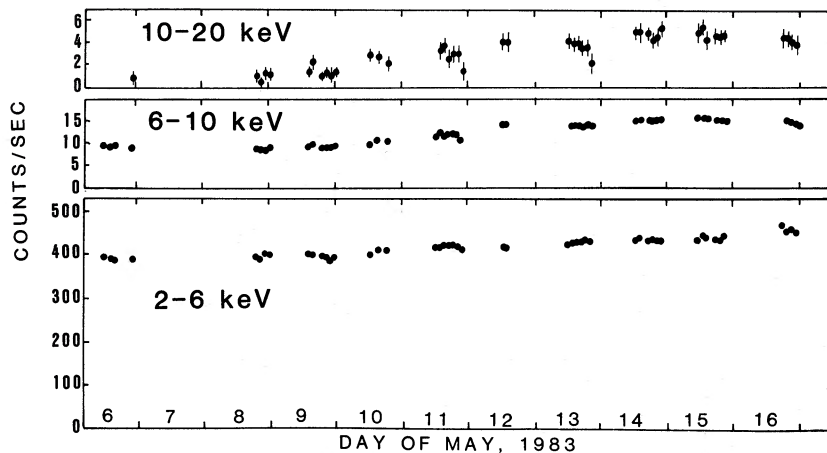


FIG. 1.—The three-color X-ray light curve of GX 339–4 during the present *Tenma* observations. Each data point refers to the photon flux for an effective area of  $640 \text{ cm}^2$ , averaged over about 20 minutes. The statistical plus systematic errors associated with the 2–6 keV and 6–10 keV data points are much smaller than the plotting symbols. The Crab intensity corresponds to  $\sim 1010 \text{ counts s}^{-1}$  in 2–6 keV,  $\sim 320 \text{ counts s}^{-1}$  in 6–10 keV, and  $\sim 193 \text{ counts s}^{-1}$  in 10–20 keV.

no fast ( $\lesssim$  minutes) variation either in the optical or X-rays, thus confirming the conclusion of Paper I. The present results give significantly new insight into the X-ray and optical emissions from GX 339–4 in the X-ray high state.

## II. X-RAY OBSERVATIONS AND RESULTS

### a) Observations

The X-ray observation of GX 339–4 was performed with the *Tenma* GSPC from 1983 May 6 through May 16. The GSPC has an effective area of  $640 \text{ cm}^2$ , and an energy resolution improved over that of conventional proportional counters by a factor of 2. The GSPC data were acquired with a time resolution of either 15.625 ms or 2.0 s. The pulse-height information was recorded in 128 spectral channels that cover

the 1.5–35 keV energy band. Details of the instrumentation are found in Tanaka *et al.* (1984) and Koyama *et al.* (1984).

Figure 1 shows the X-ray light curve of GX 339–4 in three colors. GX 339–4 was thus in a typical “high” state, with a very soft spectrum and a high soft X-ray flux (0.3–0.4 Crab units in 2–10 keV). The 2–10 keV intensity level is about 70% that of the *Hakucho* high state in 1981 (Paper I). As found during the 1981 high state, the soft X-ray (2–6 keV) intensity during the present observations does not show variation on short or medium (minutes to hours) time scales, but does exhibit a gradual  $\sim 15\%$  increase. The flux at higher energies shows a similar, but more pronounced, increase. The data above 10 keV suggest possible variations on shorter time scales.

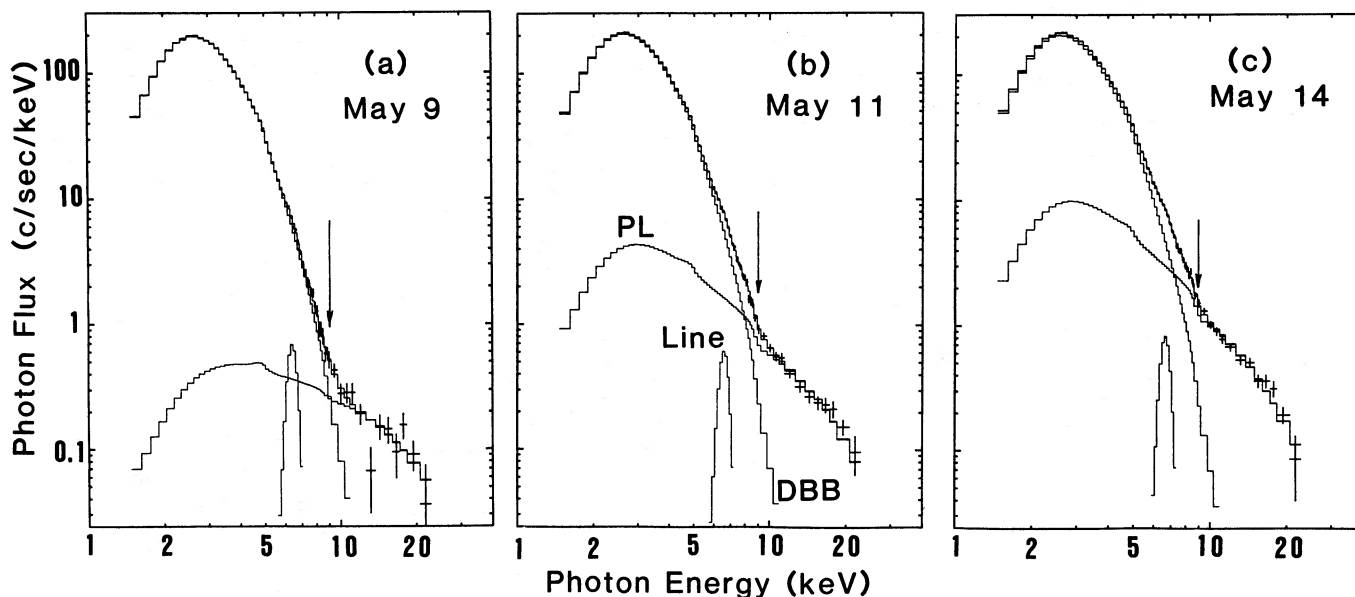


FIG. 2.—The X-ray spectra of GX 339–4 obtained with the *Tenma* GSPC, on 1983 May 9 (a), May 11 (b) and May 14 (c). The histograms show spectral model components, convolved with the detector response, to be compared with the observed data (crosses). The models include a disk-blackbody model (see text) representing the soft component (denoted DBB in b); a power-law component representing the hard tail (denoted PL); an iron emission line with its energy and intensity free parameters (denoted Line in b); K-edge absorption at 8.8 keV due to helium-like iron atoms (indicated by arrows); and neutral absorption. The best-fit model parameters are summarized in Table 2.

## b) X-Ray Spectrum

In Figure 2 we show typical examples of the GSPC pulse-height spectra of GX 339-4, taken on three occasions during the present observations. They comprise a bright soft component and a distinct hard-tail component. Note that this is the first clear detection of hard tail from GX 339-4 during a high state, though it was suggested by the *Ariel 6* (Ricketts 1983) and *OSO 8* (Robinson-Saba 1983) results. The three spectra differ little below  $\sim 10$  keV. However, the hard tail becomes more prominent toward the later phases of the observation. This corresponds to the gradual increase in the 10-20 keV flux seen in Figure 1.

Clearly, no single model spectrum of conventional form (including power-law, thin-thermal, and blackbody) can describe these concave-shaped spectra. We therefore fit the spectra with two model components (plus neutral absorption). We used a power-law model to represent the hard-tail part. For the soft component, we employed four different models, each with two free parameters: a power-law model, a thin-thermal model with Gaunt factor, a blackbody model, and a "disk-blackbody" model. The disk-blackbody (DBB) model (Pringle 1981; Mitsuda *et al.* 1984; Hoshi 1984) describes emission from an optically thick accretion disk observed at an inclination angle  $i$ . As shown in the Appendix, it is expressed as a particular superposition of multicolor blackbody elements, with two parameters:  $r_{\text{in}}(\cos i)^{1/2}$ , where  $r_{\text{in}}$  is the innermost radius of the optically thick accretion disk, and  $T_{\text{in}}$ , the blackbody temperature there.

The results of these two-component fits are shown in Table 1. The best-fit parameters for the soft component are generally consistent with previous high-state measurements (Markert *et al.* 1973; Chiapetti 1981; Ricketts 1983; Paper I), showing its unusual softness among the galactic X-ray binaries (White and Marshall 1984). The photon index for the hard tail turned out to be about  $-2$ . This value is close to those describing the low-state spectra of GX 339-4:  $-1.77 \pm 0.16$ , 10-100 keV, in 1977 August-September (Nolan *et al.* 1982);  $-1.5 \pm 0.05$ , 1-50 keV, in 1981 May (Ricketts 1983; Motch *et al.* 1983);  $-1.74 \pm 0.04$ , 1-22 keV, in 1981 June (Paper I);  $-1.58$  over

the optical to X-ray range (Motch *et al.* 1984). We therefore suggest that the hard tail in the high state is similar in nature to the entire low-state spectrum. As already pointed out previously (e.g., White, Fabian, and Mushotzky 1984; Motch *et al.* 1984), these values for GX 339-4 are similar to the low-state photon index of Cyg X-1 (about  $-1.7$ ; Oda 1977 and Liang and Nolan 1984) and of active galactic nuclei.

Among the four soft-component models, we favor the DBB model best, for the following reasons. First, it gives a significantly better fit to the observed data than the others. Second, it is accompanied by the clearest physical picture, as mentioned above and in the Appendix. Finally, the four models differ significantly below  $\sim 3$  keV in their source forms, requiring different values of  $N_{\text{H}}$ . Among the four models the DBB model gives the value of  $N_{\text{H}}$  ( $7 \times 10^{21} \text{ cm}^{-2}$ ) which is most consistent with the more reliable value,  $5 \times 10^{21} \text{ cm}^{-2}$ , obtained with the very soft X-ray experiment on board *Hakucho* (Hayakawa 1981a). Furthermore, the estimated color excess of  $E_{B-V} = 0.7-1.0$ , or  $A_V = 2-3$  (Grindlay 1979; Motch *et al.* 1984) for the optical counterpart, in combination with the empirical  $N_{\text{H}}$  versus  $E_{B-V}$  relation (Gorenstein 1975; Ryter, Cesarsky, and Audouze 1975), gives a very close value,  $N_{\text{H}} = (4-9) \times 10^{21} \text{ cm}^{-2}$ . We thus adopt the DBB model as a working hypothesis.

The DBB model, however, still fails to give a formally acceptable fit. The discrepancy is prominent around 5-8 keV. As shown in Table 2, the fit was improved significantly by the inclusion of an emission line at  $\sim 6.6$  keV (represented by a Gaussian component) and a K-edge absorption feature at  $\sim 8.8$  keV, both attributable to the helium-like (or somewhat less ionized) iron atoms. This best-fit model combination is shown in Figure 2. The line flux and the equivalent width are similar to the values for low-mass neutron star binaries (Suzuki *et al.* 1984). However, the line parameters may be quite sensitive to the choice of the continuum model, because of the steep gradient over the energy range of interest.

In Figure 3, we present the half-day averages of the spectral parameters of GX 339-4 in terms of the DBB plus power-law model. It shows that the soft component was stable both in size and temperature, while the hard tail gradually increased in intensity. This is consistent with Figure 1.

TABLE 1  
COMPARISON OF VARIOUS MODELS APPLIED TO SPECTRUM (b) OF FIGURE 2<sup>a</sup>

PARAMETER	MODEL			
	Power-Law	Thin-Thermal	Blackbody	Disk-Blackbody
Soft component:				
Scale .....	$240 \pm 11^b$	$6.8 \pm 0.2^c$	$14.5 \pm 0.1^d$	$18.4 \pm 0.2^e$
Temperature (keV) .....	...	$1.380 \pm 0.005$	$0.63 \pm 0.01$	$0.791 \pm 0.004$
Photon index .....	$5.2 \pm 0.1$	...	...	...
Hard component (Power Law):				
Scale ( $10^{-2} \text{ photons s}^{-1} \text{ cm}^{-2} \text{ keV}^{-1}$ ) .....	$2 \pm 1$	$0.04 \pm 0.02$	$13 \pm 1$	$9 \pm 4$
Photon index .....	$(-2.0)^f$	$-0.05 \pm 0.1$	$(-2.0)^f$	$-2.0 \pm 0.2$
$N_{\text{H}}$ ( $10^{21} \text{ cm}^{-2}$ ) <sup>g</sup> .....	$54.6 \pm 2.6$	$22.7 \pm 2.4$	$< 3$	$7.2 \pm 2.5$
Reduced $\chi^2$ .....	56.0	4.79	16.3	3.26
Degrees of freedom .....	60	59	60	59

<sup>a</sup> Quoted uncertainties are single-parameter 90% confidence limits.

<sup>b</sup> In unit of photons  $\text{s}^{-1} \text{ cm}^{-2} \text{ keV}^{-1}$ .

<sup>c</sup> Emission measure in unit of  $10^{60} \text{ cm}^{-3}$  at an assumed distance of 4 kpc.

<sup>d</sup> Effective blackbody radius in unit of km, at a distance of 4 kpc.

<sup>e</sup>  $r_{\text{in}}(\cos i)^{1/2}$  in unit of km, with  $i$  the inclination angle, at an assumed distance of 4 kpc.

<sup>f</sup> Fixed at  $-2.0$  to ensure a stable fitting convergence.

<sup>g</sup> Errors include systematic uncertainty in the low-energy cutoff of the detectors.

<sup>h</sup> Taking into account systematic errors.

TABLE 2  
IMPROVED MODEL FITTING TO THE THREE SPECTRA OF FIGURE 2<sup>a</sup>

PARAMETER	SPECTRUM		
	<i>a</i>	<i>b</i>	<i>c</i>
Disk-blackbody:			
$r_{\text{in}}(\cos i)^{1/2}$ (km) <sup>b</sup> .....	20.8 ± 0.4	20.7 ± 0.4	20.5 ± 0.5
$T_{\text{in}}$ (keV) .....	0.769 ± 0.005	0.774 ± 0.005	0.773 ± 0.006
Power law:			
Scale ( $10^{-2}$ photons $\text{s}^{-1} \text{cm}^{-2} \text{keV}^{-1}$ ) .....	0.3 ± 0.4	11 ± 4	28 ± 10
Photon index .....	-0.9 ± 0.5	-1.9 ± 0.2	-2.1 ± 0.2
Emission Line <sup>c</sup> :			
Line energy (keV) .....	6.45 ± 0.15	6.59 ± 0.10	6.69 ± 0.10
Line flux ( $10^{-4}$ photons $\text{s}^{-1} \text{cm}^{-2}$ ) .....	4.6 ± 2.2	3.6 ± 2.2	5.9 ± 3.0
Equivalent width (eV) .....	49 ± 25	31 ± 18	42 ± 21
$N_{\text{Fe}^{+24}}$ ( $10^{19} \text{cm}^{-2}$ ) <sup>d</sup> .....	0.7 ± 0.6	2.1 ± 0.7	2.1 ± 0.6
$N_{\text{H}}$ ( $10^{21} \text{cm}^{-2}$ ) .....	9.5 ± 2.5	8.9 ± 2.5	7.1 ± 2.6
Reduced $\chi^2$ <sup>e</sup> .....	1.63	1.71	1.53

<sup>a</sup> Quoted uncertainties are single-parameter 90% confidence limits.

<sup>b</sup> At an assumed distance of 4 kpc (see text), with  $i$  the inclination angle of the source.

<sup>c</sup> Represented by a Gaussian model of 0.1 keV FWHM.

<sup>d</sup> Column density corresponding to the 8.8 keV K-edge depth.

<sup>e</sup> For 56 degrees of freedom, and taking into account systematic errors.

### c) X-Ray Time Variation

Using the 2–10 keV X-ray data with the higher time resolution (15.625 ms), we searched for possible variability over a time scale range of 15.6 ms to  $\sim 20$  minutes. We made use of Fourier analyses, autocorrelation functions and the variation function method (a sort of variance analysis; Paper I). However, no variation, periodic or aperiodic, was found in

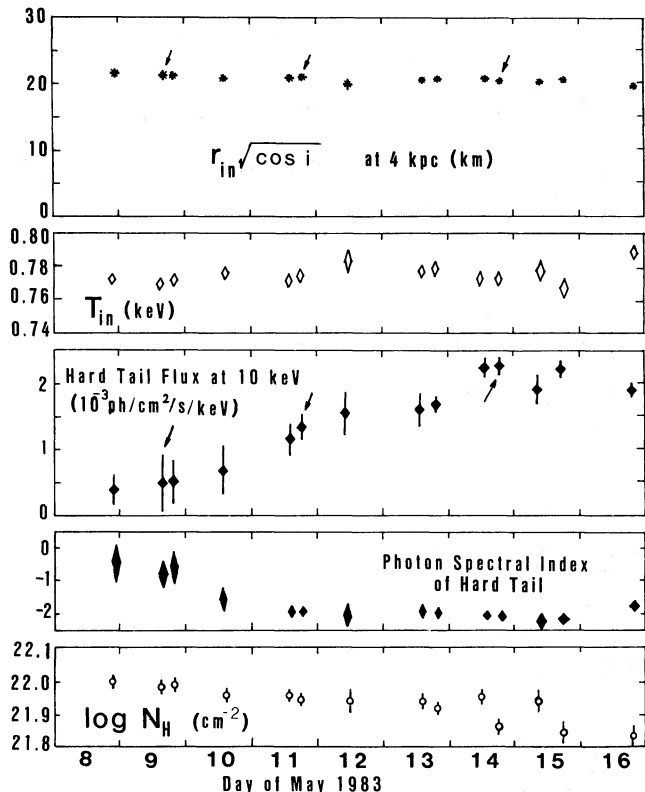


FIG. 3.—Half-day averages of the spectral parameters for the soft and hard X-ray components. The spectral model is the same as is used in Fig. 2 and Table 2. The three spectra of Fig. 2 are indicated by arrows.

excess of the Poisson noise. Inclusion of the lower time-resolution data did not alter the situation. This is clearly seen in the 2–10 keV variation function, defined in Paper I and shown in Figure 4. We estimate the upper limit to the 2–10 keV flickering fraction to be  $\sim 3\%$  (assuming continuous flickering) on any time scale between 15.6 ms and  $\sim 20$  minutes. This result confirms the conclusion of Paper I, and the reports by Li, Clark, and Rappaport (1978) and Ricketts (1983), that the rapid X-ray variability of GX 339–4 is absent in the high state.

We also carried out time series analyses at higher energy bands, to search for variability in the hard-tail part of the spectrum. However, we could not obtain meaningful results because of the poor signal-to-noise ratio above  $\sim 10$  keV. We quote an upper limit of  $\sim 40\%$  to the 10–20 keV flickering fraction on any time scale between 15.6 ms and  $\sim 20$  minutes. This upper limit is similar to the actually observed flickering level in the low state (Paper I). Thus we cannot determine whether or not the hard tail detected during the present observation had variability characteristics similar to those of the flickering X-ray emission in the low state.

### III. OPTICAL OBSERVATIONS AND RESULTS

Optical photometry and monitoring of GX 339–4 were undertaken on several occasions between 1983 May 11–16 on the 1.0 m telescope at Siding Spring Observatory. The Two Channel Chopper (TCC; Bessel 1985) was used in both a dual channel chopping mode (1P21 and S20 photo multipliers), and in a single channel, non chopping mode (1P21 photomultiplier). The latter mode provided the time series data discussed below. All of the photometric data were obtained in clear conditions, with  $1''$ – $3''$  seeing an instrument aperture of  $10''$ – $20''$  diameter. A brief spectrum of GX 339–4 was also obtained on May 18 with the Anglo-Australian Telescope (AAT). It is presented in Figure 5. It shows the H $\alpha$  and He II ( $\lambda 4686$ ) emission lines reported by Grindlay (1979), and contributed additional color measurements.

The optical photometry is summarized in Table 3. The object was relatively bright,  $V \approx 16.4$ , compared to the extreme range of reported magnitudes:  $B > 21$  (Ilovaisky

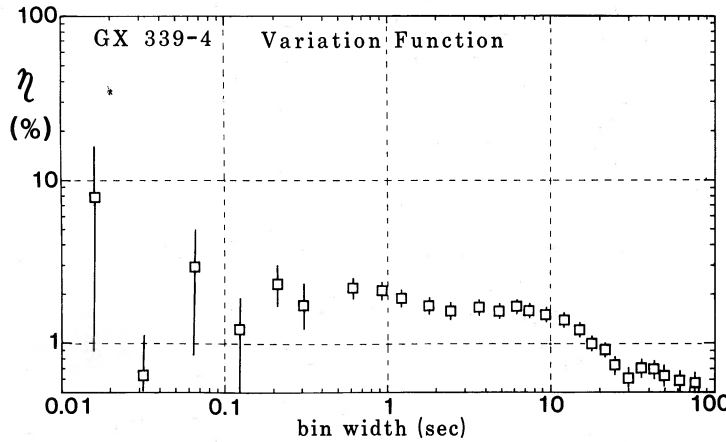


FIG. 4.—The 2–10 keV variation function of GX 339–4 based on the integration time of about 8,800 s. As described in detail in Paper I, the variation function expresses the intrinsic rms percentage variation as a function of the data binning. This figure shows that the 2–10 keV intrinsic variation of GX 339–4 was  $\leq 3\%$  on any time scale between 15.6 ms and 100 s. A structure near 20–30 s is due to the spacecraft spin (with a period of about 30 s) which slightly modulates the source flux.

and Chevalier 1981) and  $V = 15.4$  (MIC). The magnitudes and colors are comparable to those reported at the time of the optical identification ( $V = 16.7$ ,  $B - V = 0.84$ ,  $U - B = -0.24$ ; Doxsey *et al.* 1979 and Grindlay 1979). A small night-to-night variation in  $V$  is present, as are significant changes in color;  $B - V$  reddens with time, while  $U - B$  varies erratically. We note that the source was about 1 mag brighter than these results when it exhibited the rapid (down to  $\sim 10$  ms) aperiodic variability reported by MIC.

Time series measurements of GX 339–4 were obtained on May 11, 1514–1720 UT using integration times of 1.0 s and 100 ms. The 1.0 s data consist of seven segments in  $U$ ,  $B$ , and  $V$  acquired over a total time of  $\sim 25$  minutes, with a comparable time devoted to sky measurements. These data provided the  $UBV$  magnitudes included in Table 3. The 100 ms data on May 11 were accumulated for 15 minutes using a  $V$  filter. Time series data were also acquired on May 15, 1527–1602 UT with a resolution of 1.0 s. No filter was used, and GX 339–4 was observed for a total of  $\sim 24$  minutes, and the sky for  $\sim 6$  minutes.

TABLE 3

OPTICAL PHOTOMETRY OF GX 339-4

Date	$V$	$U - B$	$B - V$	$V - R$
1967 May 11 ...	$16.56 \pm 0.04$	$-0.13 \pm 0.05$	$0.77 \pm 0.04$	...
1962 May 12 ...	$16.26 \pm 0.07$	$-0.31 \pm 0.04$	$0.81 \pm 0.03$	...
1964 May 15 ...	$16.36 \pm 0.06$	$-0.07 \pm 0.06$	$1.05 \pm 0.04$	...
1979 May 18 <sup>a</sup> ...	...	$-0.20 \pm 0.10$	$1.00 \pm 0.10$	$0.52 \pm 0.10$
Average .....	16.39	-0.18	0.91	...

<sup>a</sup> From AAT spectrum.

The unfiltered data on May 15 provided the best signal-to-noise ratio for time series analysis; source and sky count rates were  $\sim 117$  counts  $s^{-1}$  and  $\sim 229$  counts  $s^{-1}$ , respectively. A straightforward comparison of the variances shows a possible excess variance over that expected from Poisson statistics. The fractional source count rate associated with this flickering is calculated to be  $6.9\% \pm 3.7\%$ , for continuous flickering at a 1.0 s time scale, where the error is the rms of three independent determinations. The sky data (which contributed  $\sim \frac{2}{3}$  of the

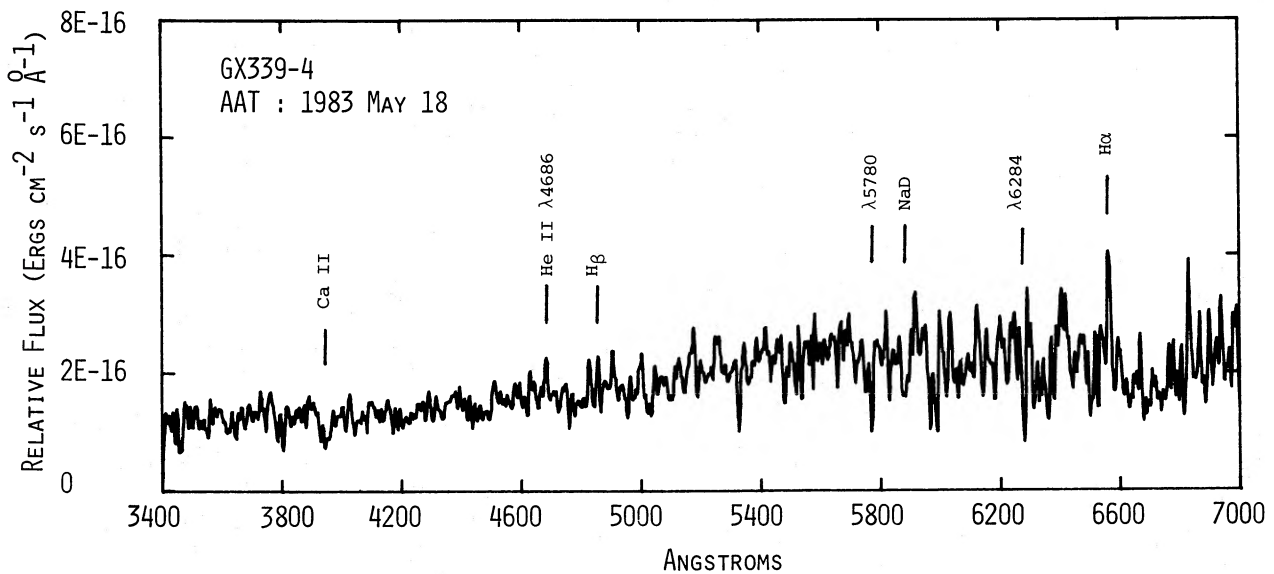


FIG. 5.—Optical spectrum of GX 339–4 obtained with the Anglo-Australian Telescope on 1983 May 18. The integration time was 500 s. Significant emission lines and interstellar absorption features are indicated.

source + sky signal) were well behaved statistically, but since we cannot rule out all possible systematic effects, we quote an upper limit of 14% for the flickering fraction. An autocorrelation analysis was also performed on the 1.0 s data of May 15 (1196 1.0 s bins), and found to show no aperiodic behavior. The 20 s feature reported by MIC is absent, although with the reported full amplitude of 30%–40%, it should have been easily detectable. The plot of our data would also clearly exhibit individual 20 s flares of this amplitude, but none are present.

The variance analysis was also performed on the limited 1.0 s data of May 11. No significant flickering, or individual  $\sim 20$  s flares, were detected in any of the wavebands measured. We calculate a  $2\sigma$  upper limit of 15% for the flickering fraction on this occasion.

The 100 ms data of May 11 ( $V$  filter) have count rates of 4 counts per bin and 11 counts per bin for source and sky, respectively. The brightest 10–20 ms flares seen in Figure 3 of MIC would amount to a factor of  $\sim 2$  increase when averaged over 100 ms. This would be only a  $2\sigma$  effect in our data. A  $\chi^2$  test indicates that our data do in fact exhibit a slight excess variance, corresponding to a flickering fraction of 40% and 28% in two measures. Due to limited time, we were unable to measure a standard star or sky with 100 ms time resolution. Any non-statistical behavior would reduce the flickering value for the source. Thus we quote an upper limit of  $\sim 50\%$  on the flickering fraction for our 100 ms data. This appears to be consistent with the flickering level at 10–20 ms in Figure 3 of MIC.

In conclusion, our 1.0 s data clearly do not exhibit the dramatic 30%–40% full amplitude  $\sim 20$  s flaring observed by MIC when GX 339–4 was  $\sim 1$  mag brighter ( $V \approx 15.4$ ). Our limited 100 ms data do not allow us to state unambiguously whether or not the 10–100 ms flaring reported in MIC was present.

#### IV. DISCUSSION

##### a) X-Ray and Optical Correlation

The present simultaneous observations in the X-ray high state have shown that the optical counterpart was *fainter* ( $V \approx 16.4$ ) by about 1 mag as compared to the 1981 X-ray low state ( $V \approx 15.4$ ; MIC), indicating a negative correlation between the optical and soft X-ray intensities. It was also shown that the rapid variability was absent both in X-rays and visible light. These features agree well with the previous X-ray (Paper I) and optical (Motch *et al.* 1984) results and confirm that the clear bimodal behavior exists both in X-rays and in visible light.

In Table 4 we show the X-ray and optical energy fluxes calculated from the present observations. On this occasion we also note that the energy flux scale of Figure 3b of Paper I was incorrect and should be reduced by a factor 4.

##### b) Soft X-Ray Emission

Mitsuda *et al.* (1984) and Hoshi (1984) successfully described the X-ray spectra of the low-mass neutron star binaries (LMB) as a superposition of two spectral components; a harder 2 keV blackbody which varies on a time scale of minutes to hours, and a softer, stable, disk-blackbody with  $T_{\text{in}} \approx 1.4$  keV and  $r_{\text{in}} \approx 20$  km. The former component is identified with optically thick emission from near the neutron star surface, while the latter with the emission from the optically thick accretion disk. The innermost disk region, intervening between these two

TABLE 4

OPTICAL AND X-RAY ENERGY FLUX DURING THE PRESENT OBSERVATIONS

Parameter	Observed Flux <sup>a</sup> (ergs s <sup>-1</sup> cm <sup>-2</sup> )	Luminosity <sup>b</sup> (ergs s <sup>-1</sup> )
Soft X-ray (2–10 keV) <sup>c</sup> .....	$6.8 \times 10^{-9}$	$6.4 \times 10^{36}/\cos i$
Hard X-ray (10–20 keV) <sup>d</sup> ...	$(0.8\text{--}3.2) \times 10^{-10}$	$(1.5\text{--}6.0) \times 10^{35}$
Optical (300–700 nm) <sup>d</sup> .....	$5.0 \times 10^{-11}$	$1.0 \times 10^{35}$
Bolometric flux <sup>e</sup> .....	$2.0 \times 10^{-8}$	$1.9 \times 10^{37}/\cos i$

<sup>a</sup> Corrected for the interstellar absorption and reddening, assuming  $N_{\text{H}} = 5 \times 10^{21}$  cm<sup>-2</sup> and  $A_{\text{v}} = 2.5$ .

<sup>b</sup> At an assumed distance of 4 kpc (see text).

<sup>c</sup> Assuming a disklike emission with the inclination angle  $i$ .

<sup>d</sup> Assuming spherical emission.

<sup>e</sup> For the disk-blackbody component only, integrating over the entire energy range.

emission regions, may be optically thin and may play a subsidiary role in X-ray emission through Comptonization.

Let us now replace the neutron star in the above model by a black hole of mass  $M_{\text{x}}$  (Tanaka 1983; Makishima 1984). Then the disappearance of the variable harder component will make the overall spectrum considerably softer, and very stable in time. This agrees with the basic X-ray properties of GX 339–4 in the high state. In addition, the disk around a black hole becomes dynamically unstable at  $r \lesssim 3R_{\text{s}} = 9 \times 10^5 (M_{\text{x}}/M_{\odot})$  cm (with  $R_{\text{s}} = 2GM_{\text{x}}/c^2$  the Schwarzschild radius). For  $M_{\text{x}} \gtrsim 3 M_{\odot}$  this effect will determine  $r_{\text{in}}$  (before the disk is destabilized by the radiation pressure), thus increasing  $r_{\text{in}}$  noticeably and decreasing  $T_{\text{in}}$  correspondingly. This is just what we have observed: the value  $T_{\text{in}} \approx 0.77$  keV (Tables 1 and 2; Fig. 3) is significantly lower than the typical value  $T_{\text{in}} = 1\text{--}1.4$  keV for the LMB (Mitsuda *et al.* 1984), although these values are subject to the modeling of an accretion disk corona (Hirano *et al.* 1984).

Thus the DBB model gives unified description of the observed soft X-ray emission from GX 339–4 in terms of an accreting black hole. This also gives a theoretical basis to the “ultra soft spectrum” criterion for the high-state black hole binaries (White, Kaluzienski, and Swank 1984; White and Marshall 1984). Note that the meaning of “ultra-softness” in our interpretation is twofold: an accreting high-state black hole lacks the harder (2 keV blackbody) component, and in addition it can have a lower value of  $T_{\text{in}}$  than the LMB.

In this context, we notice that the high-state X-ray spectrum of Cyg X-1 also comprises a very soft component, with a typical blackbody temperature of  $\sim 0.38$  keV and a blackbody radius of  $\sim 70$  km (Robinson-Saba 1983; Chiapetti *et al.* 1981; Bedford *et al.* 1981) for an assumed distance of 2.5 kpc. If we use the DBB model instead then we would obtain  $T_{\text{in}} \approx 0.38/0.71 \approx 0.53$  keV (Appendix and Fig. 6) and  $r_{\text{in}} \sim 70$  km, since Cyg X-1 has a small inclination angle (Bolton 1975). Identifying  $r_{\text{in}}$  with  $3R_{\text{s}}$  we obtain  $M_{\text{x}} \sim 8 M_{\odot}$  for the compact object in Cyg X-1; this agrees nicely with the currently accepted value (e.g., Liang and Nolan 1984), and supports the DBB interpretation.

##### c) Optical Emission

The optical emission from GX 339–4 in the X-ray low state, which is violently variable (MIC), may be a cyclotron emission in a thin hot plasma around a black hole (Fabian *et al.* 1982; cf. Apparao 1984). However, the optical emission mechanism in the X-ray high state seems fundamentally different.

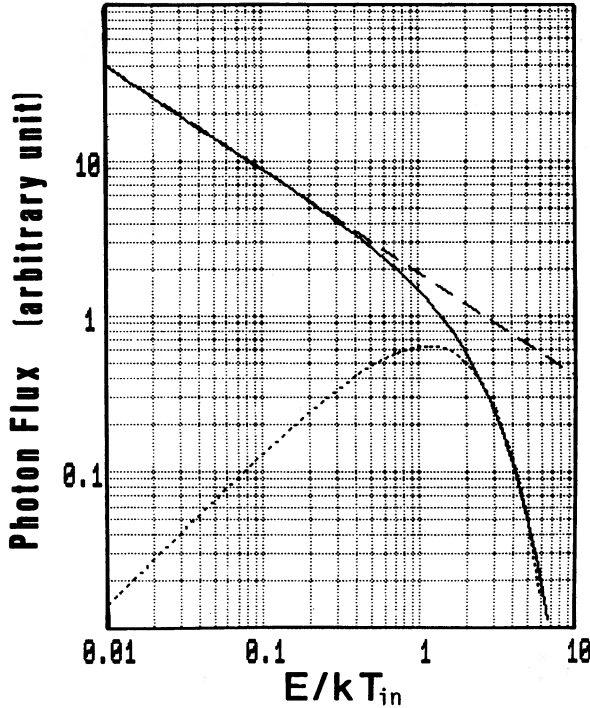


FIG. 6.—The disk-blackbody (DBB) photon spectrum as a function of  $E/k_B T_{in}$ , under the assumption of  $T_{out}/T_{in} \ll 0.1$ . Here  $E$  is the emitted photon energy. For comparison, a power-law spectrum of photon index  $-2/3$  (dashed line), and a blackbody photon spectrum with a temperature  $T_{bb} = 0.71 T_{in}$  (dotted curve), are also shown.

The optical parameters of GX 339-4 we observed may be compared with those of the LMB (van Paradijs 1980; Bradt and McClintock (1983). Assuming an interstellar extinction of  $A_v \approx 2.5$  (Grindlay 1979; Motch *et al.* 1984), and using the standard relations  $A_v = 3E_{B-V}$  and  $E_{U-B} = 0.72E_{B-V}$ , we estimate from Table 3 the time-averaged intrinsic colors as  $U-B = -0.78$  and  $B-V = 0.08$ . These values are very similar to the “canonical” parameters for the LMB,  $U-B = -0.95$  and  $B-V = 0.03$  (van Paradijs 1980). Next, we derive from Table 4 the X-ray (2–10 keV) to optical (300–700 nm) energy flux ratio of about 140. This is comparable to, or slightly smaller than, those of the LMB. (This ratio is about 20 in the low state; Motch *et al.* 1983.) Furthermore, the spectral features of GX 339-4, such as emission lines superposed on a flat continuum (Fig. 5; Grindlay 1979), resemble those of the LMB. We thus presume that the optical emission from GX 339-4 in the high state is quite similar in mechanism to those from the LMB.

The optical emission from the LMB is considered to originate through X-ray reprocessing at the outer (e.g.,  $r > 10^9$  cm) disk surface, where X-ray heating dominates the viscous heat generation (Hayakawa 1981b; Hoshi 1984). This emission dominates the intrinsic optical emission (at the low-energy end of the DBB spectrum) from the optically thick disk. Since the outer disk structure should differ little between the LMB and a black hole binary, we presume that the optical emission from the high-state GX 339-4 must be of the same origin. The absence of fast optical variation in the high state is consistent with this interpretation.

#### d) Distance, Mass, and Luminosity of GX 339-4

Following the above discussion, we can estimate the distance of GX 339-4 by scaling the observed optical magnitude

( $V = 16.4$  on the average) against the “standard” absolute magnitude,  $M_v = 1.2$  (van Paradijs 1980), for the LMB. Assuming again  $A_v \approx 2.5$  we get a distance of about 3.5 kpc. This value is in agreement with the previous estimate of  $\sim 4$  kpc, derived by Doxey *et al.* (1979) on the assumption that GX 339-4 and Cyg X-1 have the same X-ray luminosity. We therefore express the distance of GX 339-4 as  $4 \times D_4$  kpc, with a working hypothesis of  $D_4 \approx 1$ .

This distance estimate was already used in Figure 3 and Table 2 to derive the relation  $r_{in}(\cos i)^{1/2} \approx 21D_4$  km from the observed DBB flux. Equating this with  $3R_s$ , we obtain  $M_x \approx 2.3D_4(\cos i)^{1/2} M_\odot$  for the mass of the compact object in GX 339-4. This value of  $M_x$  is self-consistent within the black hole hypothesis.

From the above  $r_{in}$  and the observed  $T_{in} \approx 0.77$  keV, we can calculate the bolometric luminosity of the DBB component as

$$L_x = 4\pi r_{in}^2 \sigma T_{in}^4 = 1.9 \times 10^{37} D_4^2 / \cos i \\ = 4.3 \times 10^{37} D_4^2 \cdot \beta^2 \text{ ergs s}^{-1},$$

where  $\beta = (2/3)/(\cos i)^{1/2} \approx 1$  represents a typical aspect effect and  $\sigma$  is the Stefan-Boltzmann constant (see the Appendix). This result is listed in Table 4. This  $L_x$  may be slightly smaller than the high-state luminosity of Cyg X-1 ( $\sim 6 \times 10^{37}$  ergs  $s^{-1}$ ; Liang and Nolan 1984).

Finally, the mass accretion rate,  $\dot{M}$ , can be calculated via the relation  $L_x = g^2 G M M_x / 2r_{in}$ , where  $g = [1 - (R_s/r)]^{1/2}$  is the correction for the general relativity and the factor  $1/2$  reflects the fact that half the gravitational energy release is swallowed into the black hole. Identifying  $r_{in}$  with  $R_s$  we have

$$\dot{M} = 3.7 \times 10^{17} D_4^2 / \cos i = 8.3 \times 10^{17} D_4^2 \cdot \beta^2 \text{ g s}^{-1}.$$

#### e) Hard X-Ray Tail

The present X-ray observation established the presence of hard X-ray tail in the high state spectra of GX 339-4. We notice that very similar hard tails were observed in several “ultra soft” X-ray transients, including Nova Ophiuchi (Wilson and Rothschild 1983), H1743-32 and A0620-00 (White, Kaluzienski, and Swank 1983). Recently the compact object in A0620-00 was shown to have a mass lower limit of  $\sim 3 M_\odot$  (McClintock and Remillard 1986), thus being a very promising black hole candidate. This strongly reinforces the black hole candidacy of GX 339-4. The hard X-ray tail we observed may be interpreted naturally as due to the Comptonization in the optically thin, hot, inner disk region (e.g., Liang and Nolan 1984, and references therein). Such a hard tail may also be present in the LMB, but the absence of the 2 keV blackbody component in the black hole binaries will make the hard tail far more noticeable.

In the present case, we assume that the source photons for the Compton process are provided by the DBB component itself. The apparent kink (at  $\sim 10$  keV; see Fig. 2) between the soft and hard X-ray components indicates that only a small fraction of the DBB photons undergoes Comptonization. Then, the situation can be specified by this fraction  $f$ , and by the temperature  $T_e$ , density  $n_e$ , and size  $r_e$  of the Comptonizing hot plasma.

Assuming again  $r_e \approx r_{in} \approx 3R_s$ , the plasma density at  $r = r_{in}$  can be estimated from the relation  $\dot{M} = 4\pi r_{in}^2 n_e m_p v_{in}(h/2r_{in})$ , where  $h$  is the full disk thickness,  $v_{in} \approx 10^{10}$  cm  $s^{-1}$  is the disk infall velocity ( $\sim$  free-fall velocity) at  $r = 3R_s$ , and  $m_p$  is the proton rest mass. If we assume  $h \approx r_{in}$  then all the dependence on distance, inclination, and black hole mass cancels out, to

give

$$n_e \approx 8 \times 10^{17} \text{ cm}^{-3}$$

Using the Thomson cross section  $\sigma_T$ , the Compton opacity then becomes

$$\tau = n_e r_{in} \sigma_T = 1.8 \times D_4 \beta,$$

where  $\beta = (\frac{2}{3})/(\cos i)^{1/2}$  is the same as before.

Next, the power-law photon index of about  $-2.1$  can be combined with the spherical model of Sunyaev and Titarchuk (1980) to get

$$(k_B T_e/m_e c^2)(\tau + \frac{2}{3})^2 \approx 0.73,$$

where  $k_B$  is the Boltzmann constant and  $m_e$  is the electron rest mass. From the above two equations and assuming  $D_4 \beta \approx 1$ , we obtain

$$k_B T_e \approx 115/(0.37 + D_4 \beta)^2 \approx 60 \text{ keV}.$$

These values for  $\tau$  and  $T_e$  are similar to those for Cyg X-1 (e.g., Liang and Nolan 1984 and references therein) and Nova Ophiuchi (Wilson and Rothschild 1983). Finally, the luminosity ratio between hard and soft X-ray components from Table 4,  $L_{\text{hard}}/L_{\text{soft}} = (0.02-0.09) \cos i$ , can be substituted into the net energy transfer relation

$$L_{\text{hard}}/L_{\text{soft}} \approx (k_B T_e/m_e c^2)\tau f$$

to yield  $f \approx (0.02-0.1)\beta D_4^{-1}(0.37 + D_4 \beta)^2 \approx 0.1$ . This seems a reasonable value for the geometrical probability of a DBB photon to interact with the hot inner torus. The gradual increase in the hard tail flux may be due to changes in this geometry. Thus the observed hard tail is satisfactorily described in terms of the Comptonization of soft X-ray photons by a plasma of  $\sim 60$  keV temperature.

#### f) High-Low Transitions

The X-ray low state is usually interpreted as the case when the optically thin hot disk extends far out radially (e.g., Liang and Nolan 1984). Most of X-rays then arise from Comptonization, as described above, and the flickering optical radiation may be due to thermal cyclotron emission (Fabian *et al.* 1982). The high-to-low transition of the source may occur in response to a slight decrease in the mass accretion rate, via thermal instability (Ichimaru 1977), via Compton cooling feedback mechanism (Guilbert and Fabian 1982), or via decrease in the electron-positron pair creation opacity (White, Fabian, and Mushotzky 1984). Whatever the mechanism, the bimodal

behavior of GX 339-4 is likely to be a manifestation of the disk transition between the optically thick and optically thin configurations.

#### V. SUMMARY AND CONCLUSIONS

We observed three distinct emission components, optical, soft X-rays, and hard X-rays, from GX 339-4 in a typical high state. We interpret each of these components as arising from a characteristic region of the accretion disk. Our interpretation can be summarized as follows:

1. The compact object in GX 339-4 seems to have a mass  $\sim 3 M_\odot$  and is likely to be a black hole.
2. GX 339-4, being a black hole binary in this scenario, lacks the variable 2 keV blackbody component that would be emitted from the "solid" surface of a neutron star in the LMB. The X-ray emission from GX 339-4 in the high state is therefore extremely soft and stable in time.
3. The X-ray heated outermost (e.g.,  $r > 10^9$  cm) disk region reprocesses X-rays into optical emission. This mechanism is essentially the same as in the low-mass binaries.
4. The intermediate (e.g.,  $3 \times 10^6 < r < 10^9$  cm) disk region is optically thick and geometrically thin. The observed soft X-ray component with a "disk-blackbody" spectrum comes from this disk region.
5. The innermost (e.g.,  $r < 3 \times 10^6$  cm) disk region is dynamically unstable due to the effect of general relativity and possibly due to radiation pressure; it is optically thin and very hot ( $k_B T_e \sim 60$  keV). This region is responsible for the generation of the hard X-ray tail through Comptonization, with an optical depth of a few.

We have shown that this interpretation accounts amazingly well for the overall results of the present simultaneous observations. Probably this is one of the cases in which the standard accretion disk theory is most successful.

We thank Dr. C. Motch of Observatoire de Besançon for valuable information on the optical observations of GX 339-4, Dr. E. Fenimore of LASL for development of the spectral fitting software, and the ANU and AAO staff at Siding Spring Observatory for their support. We also acknowledge all the members of the *Tenma* team for spacecraft operation, data reduction, and discussion. This work was supported in part by NSF (INT-82-1135; AST-84-14591) and by NASA (NAS 8-27972; NAG 8-493) in the United States, and by the Grant-in-Aid for Scientific Research (60302017) from the Ministry of Education, Science, and Culture in Japan.

#### APPENDIX

##### DISK-BLACKBODY (DBB) SPECTRUM

The disk-blackbody (DBB) spectrum describes optically thick radiation from a standard, geometrically thin accretion disk around a compact object of mass  $M_x$  (see Pringle 1981 and references therein). Its relevance to the X-ray binaries was recently revived by Hayakawa (1981*b*) and Hoshi (1984) and compared closely with the observations by Mitsuda *et al.* (1984). As shown below, it is expressed as a particular superposition of multicolor blackbody components.

Let  $T(r)$  denote the local blackbody temperature of a such a disk at a distance  $r$  from the compact object. Then  $4\pi r dr \sigma T(r)^4$  gives the radiation luminosity from an annular disk element of radial thickness  $dr$ , with  $\sigma$  the Stefan-Boltzmann constant. Equating this with the energy release necessary for the disk matter to fall in by a distance  $dr$ , namely  $\frac{1}{2}G\dot{M}M_x dr/r^2$ , we obtain (Hayakawa 1981*b*)

$$T(r) = (3G\dot{M}M_x/8\pi\sigma r^3)^{1/4}.$$

Here  $G$  is the constant of gravity, and  $\dot{M}$  is the mass accretion rate. A more exact treatment (Shakura and Sunyaev 1973;

Pringle 1981) leads to

$$T(r) = [3GM\dot{M}_x/8\pi\sigma r^3]^{1/4} \cdot [1 - (r_c/r)^{1/2}]^{1/4},$$

where  $r_c$  is a critical radius (usually close to that of the compact star) within which the angular momentum is transferred inward.

The composite photon spectrum emitted from such a disk at an inclination angle  $i$  is then readily expressed as a superposition of various blackbody elements from different parts of the disk. Integrating from the innermost disk radius  $r_{in}$  out to the outermost disk radius  $r_{out}$ , and assuming  $r_{in} \gg r_c$ , we obtain the expression for the DBB spectrum as (Mitsuda *et al.* 1984);

$$f(E) = \int_{r_{in}}^{r_{out}} 2\pi r \cos i B[E, T(r)] dr = \frac{8\pi}{3} r_{in}^2 \cos i \int_{T_{out}}^{T_{in}} (T/T_{in})^{-11/3} B(E, T) dT/T_{in}.$$

Here  $T_{in} = T(r_{in})$  and  $T_{out} = T(r_{out})$  are the innermost and outermost disk temperatures, respectively;  $E$  is the emitted photon energy; and  $B(E, T)$  is the blackbody photon flux per unit photon energy from a unit surface area of temperature  $T$ . As shown in Figure 6, the DBB spectrum has the following properties:

1. Since  $T_{out}$  is usually well below the energy range of interest, the DBB spectrum is determined essentially by two parameters;  $r_{in} (\cos i)^{1/2}$ , and  $T_{in}$ .
2. For the photon energy  $E \gtrsim 2k_B T_{in}$ , the DBB spectrum is well approximated by a single blackbody spectrum with a temperature  $T_{bb} = 0.7T_{in}$ . Here  $k_B$  is the Boltzmann constant.
3. For  $k_B T_{out} \ll E \lesssim 0.3k_B T_{in}$  the DBB spectrum becomes a power-law spectrum of photon index  $-\frac{2}{3}$ , or equivalently, energy index  $\frac{1}{3}$ .
4. The total luminosity of the DBB radiation is simply  $4\pi r_{in}^2 \cdot \sigma T_{in}^4$ .

#### REFERENCES

- Apparao, K. M. V. 1984, *Astr. Ap.*, **139**, 375.  
 Bedford, D. K., Carpenter, G. F., Goodall, C. V., Pollock, A. M., Cole, R. E., Cruise, A. M., and Osborne, J. P. 1981, *Space Sci. Rev.*, **30**, 373.  
 Bessell, M. B. 1985, *Pub. A.S.P.*, submitted.  
 Bolton, C. T. 1975, *Ap. J.*, **200**, 269.  
 Bradt, H. V., and McClintock, J. E. 1983, *Ann. Rev. Astr. Ap.*, **21**, 13.  
 Chiapetti, L. 1981, *Space Sci. Rev.*, **30**, 447.  
 Chiapetti, L., Branduardi-Raymont, G., Bell Burnell, S. J., Ives, J. C., Parmar, A. N., and Sanford, P. W. 1981, *M.N.R.A.S.*, **197**, 139.  
 Cowley, A. P., Crampton, D., Hutchings, J. B., Remillard, R., and Penfold, J. E. 1983, *Ap. J.*, **272**, 118.  
 Dower, R. G., Bradt, H. V., and Morgan, E. H. 1982, *Ap. J.*, **261**, 228.  
 Doxsey, R., Grindlay, J., Griffiths, R., Bradt, H., Johnston, M., Leach, R., Schwartz, D., and Schwartz, J. 1979, *Ap. J. (Letters)*, **228**, L67.  
 Fabian, A. C., Guilbert, P. W., Motch, C., Ricketts, M., Ilovaisky, S. A., and Chevalier, C. 1982, *Astr. Ap.*, **111**, L9.  
 Gorenstein, P. 1975, *Ap. J.*, **198**, 95.  
 Grindlay, J. E. 1979, *Ap. J. (Letters)*, **232**, L33.  
 Guilbert, P. W., and Fabian, A. C. 1982, *Nature*, **296**, 226.  
 Hayakawa, S. 1981a, *Space Sci. Rev.*, **29**, 221.  
 ———. 1981b, *Pub. Astr. Soc. Japan*, **33**, 365.  
 Hirano, T., Hayakawa, S., Kunieda, H., Makino, F., Masai, K., Nagase, F., and Yamashita, K. 1984, *Pub. Astr. Soc. Japan*, **36**, 769.  
 Hoshi, R. 1984, *Pub. Astr. Soc. Japan*, **36**, 785.  
 Hutchings, J. B., Crampton, D., and Cowley, A. P. 1983, *Ap. J. (Letters)*, **275**, L43.  
 Ichimaru, S. 1977, *Ap. J.*, **214**, 840.  
 Ilovaisky, S. A., and Chevalier, C. 1981, *IAU Circ.*, 3856.  
 Koyama, K., *et al.* 1984, *Pub. Astr. Soc. Japan*, **36**, 659.  
 Li, F., Clark, G., and Rappaport, S. 1978, *IAU Circ.*, 3238.  
 Liang, E. P., and Nolan, P. L. 1984, *Space Sci. Rev.*, **38**, 353.  
 Maejima, Y., Makishima, K., Matsuoka, M., Ogawara, Y., Oda, M., Tawara, Y., and Doi, K. 1984, *Ap. J.*, **285**, 712 (Paper I).  
 Makishima, K., 1984, in *Proc. Symposium X-Ray Astronomy 84.*, ed. M. Oda and R. Giacconi (Tokyo: Institute of Space and Astronomical Science), p. 165.  
 Margon, B. 1984, *Ann. Rev. Astr. Ap.*, **22**, 507.  
 Markert, T. H., Canizares, C. R., Clark, G. W., Lewin, W. H. G., Schnopper, H. W., and Sprott, F. 1973, *Ap. J. (Letters)*, **184**, L67.  
 McClintock, J. E., and Remillard, R. A. 1986, *Ap. J.*, **308**, 110.  
 Mitsuda, K. *et al.* 1984, *Pub. Astr. Soc. Japan*, **36**, 741.  
 Motch, C., Ilovaisky, S. A., and Chevalier, C. 1982, *Astr. Ap.*, **109**, L1 (MIC).  
 Motch, C., Ilovaisky, I. A., Chevalier, C., and Angebault, P. 1984, *Space Sci. Rev.*, **40**, 219.  
 Motch, C., Ricketts, M. J., Page, C. G., Ilovaisky, S. A., and Chevalier, C. 1983, *Astr. Ap.*, **119**, 171.  
 Nolan, P. L., Knight, F. K., Levine, A. M., Lewin, W. H. G., and Primini, F. A. 1982, *Ap. J.*, **262**, 727.  
 Oda, M. 1977, *Space Sci. Rev.*, **20**, 757.  
 Pringle, J. E. 1981, *Ann. Rev. Astr. Ap.*, **19**, 137.  
 Ricketts, M. 1983, *Astr. Ap.*, **118**, L3.  
 Robinson-Saba, J. L. 1983, Ph.D. thesis, University of Maryland; and Goddard Space Flight Center Technical Memorandum 85095.  
 Ryter, C., Cesarsky, C. J., and Audouze, J. 1975, *Ap. J.*, **198**, 103.  
 Samimi, J., *et al.* 1979, *Nature*, **278**, 434.  
 Shakura, N. I., and Sunyaev, R. A. 1973, *Astr. Ap.*, **24**, 337.  
 Sunyaev, R. A., and Titarchuk, L. G. 1980, *Astr. Ap.*, **86**, 121.  
 Suzuki, K., *et al.* 1984, *Pub. Astr. Soc. Japan*, **36**, 761.  
 Tanaka, Y. 1983, in *Proc. 18th Int. Cosmic Ray Conference*, Bangalore, **12**, 91.  
 Tanaka, Y., *et al.* 1984, *Pub. Astr. Soc. Japan*, **36**, 641.  
 van Paradijs, J. 1980, *Astr. Ap.*, **103**, 140.  
 White, N. E., Fabian, A. C., and Mushotzky, R. F. 1984, *Astr. Ap.*, **133**, L9.  
 White, N. E., Kaluzienski, L. J., and Swank, J. H. 1984, in *Proc. AIP Conference on High Energy Transients in Astrophysics*, ed. S. E. Woosley (NY: AIP), p. 31.  
 White, N. E., and Marshall, F. E. 1984, *Ap. J.*, **281**, 354.  
 Wilson, C. K., and Rothschild, R. E. 1983, *Ap. J.*, **274**, 717.

H. V. BRADT and R. A. REMILLARD: Center for Space Research, Massachusetts Institute of Technology, Cambridge, Massachusetts 02139

R. HOSHI: Department of Physics, Rikkyo University, Nishi-Ikebukuro 3-Chome, Toshima-ku, Tokyo, Japan 171

Y. MAEJIMA: Micro-Electronics Laboratory, Nippon Electric Company, 4-1-1 Miyazaki, Miyamae-ku, Kawasaki, Japan 213

K. MAKISHIMA and K. MITSUDA: Institute of Space and Astronautical Science, 4-6-1 Komaba, Meguro-ku, Tokyo, Japan 153

M. NAKAGAWA: Department of Physics, Faculty of Science, Osaka City University, 3-3-138 Sugimoto, Sumiyoshi-ku, Osaka, Japan 558

I. R. TUOHY: Mount Stromlo and Siding Spring Observatories, Private Bag, Woden Post Office, ACT 2606, Canberra, Australia